

## Supporting information

# The role of halide ions in the anisotropic growth of gold nanoparticles: a microscopic, atomistic perspective

Santosh Kumar Meena,<sup>†</sup> Sirin Celiksoy,<sup>‡</sup> Philipp Schäfer,<sup>‡,¶</sup> Andreas Henkel,<sup>‡,§</sup>  
Carsten Sönnichsen,<sup>‡</sup> and Marialore Sulpizi\*,<sup>†</sup>

<sup>†</sup>*Institute of Physics, Johannes Gutenberg University Mainz, Staudingerweg 7, 55099  
Mainz, Germany*

<sup>‡</sup>*Institute of Physical Chemistry, University of Mainz, Duesbergweg 10-14, D-55128 Mainz,  
Germany*

<sup>¶</sup>*Current address: Max Planck Institute for Polymer Research, Ackermannweg 10, 55128  
Mainz, Germany*

<sup>§</sup>*Current address: Center for Data Processing (ZDV), Johannes Gutenberg University  
Mainz, Anselm Franz von Bentzel-weg 12, 55128 Mainz, Germany*

E-mail: [sulpizi@uni-mainz.de](mailto:sulpizi@uni-mainz.de)

## Solvation structure of halides

In this paragraph we report the solvation structure for the aqueous  $\text{Cl}^-$  and  $\text{Br}^-$  ions. Two systems were prepared, composed of 90  $\text{Cl}^-$  / 90  $\text{Na}^+$  and 90  $\text{Br}^-$  / 90  $\text{Na}^+$ , respectively in a box of water (Table S1). This corresponds to 1.81 M solution, as also considered in the simulations in the presence of a metal surface. After MD production run of 50 ns, trajectories from last 10 ns were analyzed to obtain the radial distribution function (RDF) of Cl-O and Br-O (Figure S1). In Figure S1, RDF of Cl-O (solid green line) and Br-O (solid orange line) as well as cumulative number (CN) for Cl-O (dotted green line) and Br-O (dotted orange line) are reported. In the case of bromide the first peak in the RDF is located at a distance of 0.322 nm and the coordination number for the first solvation shell is 6.4. These values are very close to those obtained in Car-Parrinello Molecular Dynamics (CPMD) simulations and X-ray absorption fine structure (ND+EXAFS) studies.<sup>1</sup> For chloride the first peak in the RDF is located at 0.323 nm and the coordination number for the first solvation shell is 8.6. The parameters for the chloride solvation structure obtained with the GROMOS force field can be compared to those obtained from other force fields in Ref.<sup>2</sup> and those obtained from experiments in ref.<sup>3</sup> The experimental value for the chloride coordination in the first solvation shell is around 6.<sup>3</sup> Assuming that the coordination number of chloride should change only slightly when the sodium is replaced by some other cations, experimental data from other salts can also be used, thereby getting better statistics. In this case coordination numbers as high as 11 can also be found.<sup>2</sup>

Table S1: Model details for NaCl and NaBr in water for the calculation of radial distribution function (1.81 M).

Name of System	No. of ions	No. of water molecules	Box dimensions X [nm], Y [nm] Z [nm]
NaCl solution	90 Na <sup>+</sup> , Cl <sup>-</sup>	2761	4.01, 4.01, 5.43
NaBr Solution	90 Na <sup>+</sup> , Br <sup>-</sup>	2761	4.01, 4.01, 5.43

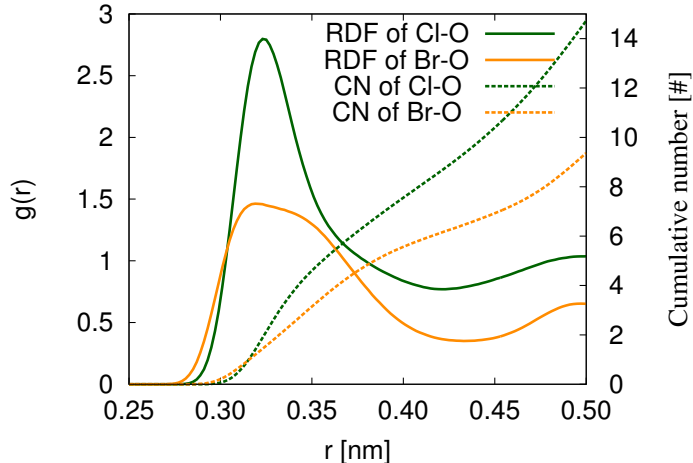


Figure S1: Cl-O (solid green line) and Br-O (solid orange line) radial distribution functions (RDF) obtained from the simulation of NaCl and NaBr in water, respectively (see system details in Table S1). Cumulative number (CN) for Cl-O (dotted green line) and Br-O (dotted orange line). The bromide-oxygen first shell distance is 0.322 nm and average first shell coordination number is 6.4. The chloride-oxygen first shell distance is 0.323 nm and average first shell coordination number is 8.6.

## Electrostatic potentials at the interface

The electrostatic potential at the gold/water interface in the presence of ions can be calculated by integrating the Poisson equation according to the following expression

$$V(z) = -\frac{1}{\epsilon_o} \int_0^z dz' \int_0^{z'} \rho(z'') dz'' \quad (1)$$

where  $\rho$  is charge density.<sup>4</sup> Both the potential  $V(z)$  and the charge density  $\rho(z)$  are functions of position along the  $z$ -axis, which is perpendicular to the gold surface and the surfactant layer. Eq.1 has already been averaged over  $x$  and  $y$  coordinates. S2d shows the electrostatic

potential for pure water, NaCl, NaBr and NaI water solution across the Au(111)/water interface.

## Halide ions on Au(111) surface in water

We have investigated the adsorption of halides for the 1.81 M, 3.87 M and 7.78 M solutions in contact with the Au(111) surface (models in Table 1 of the main text).

Figure S2 shows the normalized ion density (number density) profiles for water and ions along with the integral number of ions as a function of the distance from the Au(111) surface for 1.81 M NaCl (Figure S2a), NaBr (Figure S2b) and NaI (Figure S2c) systems. Let's first discuss the water behaviour at the gold/water interface. The red curve in Figure S2 represents the water density profile close to the Au(111) surface, which shows that for all the three solutions (NaCl, NaBr, NaI), water molecules are adsorbed in the first layer on the gold surface.

Figure S2a shows that  $\text{Cl}^-$  ions are not adsorbed significantly on the Au(111) surface (or in the subsequent layer) and remain diffused in the solution. On the other hand Figure S2b shows that  $\text{Br}^-$  ions are adsorbed on Au(111) surface and two layers are formed next to the water layer (two orange peaks near the Au(111) surface), with a larger number density in the first layer than in the second layer). Iodide ions are also adsorbed in the form of two layers (purple line in Figure S2c).

There are some interesting differences in the position of the adsorbed halide layers. In particular, the first water,  $\text{Na}^+$  and  $\text{Cl}^-$  layer adsorbed on the Au(111) surface are at 0.23 nm, 0.28 nm and 0.33 nm, respectively for NaCl solution (Figure S2a). In the case of the NaBr solution, the first water,  $\text{Na}^+$  and  $\text{Cl}^-$  layer adsorbed on the Au(111) surface is also at 0.23 nm, 0.26 nm and 0.27 nm, respectively (Figure S2b). Finally for the NaI solution the first water,  $\text{Na}^+$  and  $\text{Cl}^-$  layer adsorbed on the Au(111) surface is at 0.24 nm, 0.29 nm and 0.30 nm, respectively.

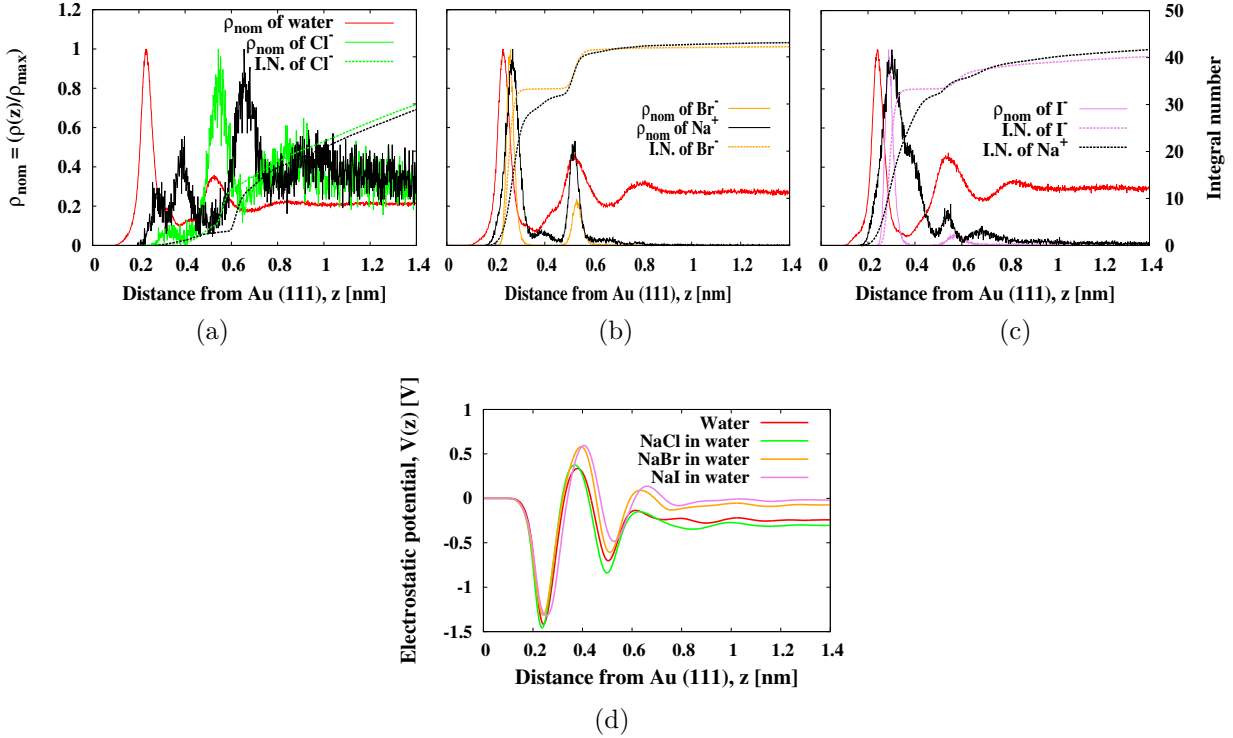


Figure S2: Normalized ion densities (number densities) of water and ions and integral numbers of ions as a function of the distance from Au(111) surface for (a) NaCl ( $\rho_{\text{max}}$  for water = 420,  $\text{Cl}^- = 3.38$ ,  $\text{Na}^+ = 3$ ), (b) NaBr ( $\rho_{\text{max}}$  for water = 339.46,  $\text{Br}^- = 62.26$ ,  $\text{Na}^+ = 29.60$ ) and (c) NaI ( $\rho_{\text{max}}$  for water = 318.14,  $\text{I}^- = 58.56$ ,  $\text{Na}^+ = 17.66$ ) in water. (d) Electrostatic potentials as a function of the distance from Au(111) surface for pure water, 1.81 M NaCl in water, 1.81 M NaBr and 1.81 M NaI in water.

The likelihood to find the halides on the gold surface can also be expressed in terms of surface density which is calculated as the integral number (I.N.) of ions in the first layer divided by surface area, and which represents the number of ions adsorbed per  $\text{nm}^2$  on the gold surface (Table S2). The number of ions in the first layer are calculated from the integral number in the first layer (see dashed lines in Figure S2a, Figure S2b, Figure S2c). From our simulation, we can evince that  $\text{Cl}^-$  has a very low propensity for the gold surface, while both  $\text{Br}^-$  and  $\text{I}^-$  show a quite high propensity for the gold surface (S2). Figure S2d shows the electrostatic potential for pure water, 1.81 M NaCl, 1.81 M NaBr and 1.81 M NaI solutions. The potential difference between Au(111) surface and water is reported in Table S3 for pure water, 1.81 M NaCl, 1.81 M NaBr and 1.81 M NaI solutions.

Table S2: Surface densities (packing densities) of  $\text{Cl}^-$ ,  $\text{Br}^-$  and  $\text{I}^-$  on Au(111) surface. The maximum standard error in the surface densities is 0.04 ions/nm<sup>2</sup>.

Name of halide	1.81 M	3.87 M	7.78 M
$\text{Cl}^-$	0.26	-	0.25
$\text{Br}^-$	2.06	2.93	3.66
$\text{I}^-$	2.07	3.38	3.61

Table S3: Electrostatic potential difference between Au(111) and the bulk water for halide ions for models in Table 1 in the main text. The maximum standard error in the potential difference is 0.01 V

Name of system	1.81 M	3.87 M	7.78 M
Pure water	0.24	-	-
NaCl in water	0.31	-	0.27
NaBr in water	0.09	0.05	-0.11
NaI in water	0.02	-0.04	0.03

Figure S3 and Figure S4 present the normalized density profiles for water and ions as well as the integral numbers (dashed lines) as a function of the distance from the Au(111) surface for the 3.87 M sodium halide (NaBr and NaI) solutions and for the 7.78 M sodium halide (NaCl, NaBr and NaI) solutions. The surface densities for 3.87 M sodium halide and 7.78 M sodium halide are reported in Table S2. The surface density of  $\text{Cl}^-$  doesn't change with the concentration, whereas the surface densities of  $\text{Br}^-$  and  $\text{I}^-$  increase with the increasing of the concentration. Figure S3c and Figure S4d show the electrostatic potential as a function of distance from the Au(111) surface for the 3.87 M and 7.78 M sodium halide solutions. The potential differences between the Au(111) surface and the bulk water, for both the 3.87 M sodium halide and 7.78 M sodium halide solutions are reported in Table S3.

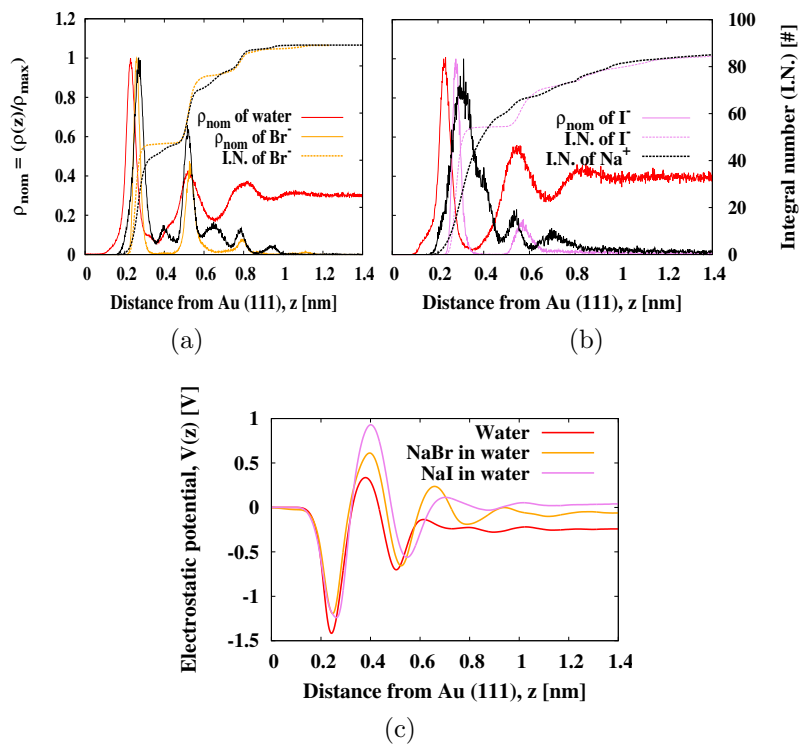


Figure S3: Normalized ion densities (number densities) of water and ions and integral numbers of ions as a function of the distance from Au(111) surface for 3.87 M (a) NaBr ( $\rho_{\text{max}}$  for water = 296.28, Br<sup>-</sup> = 76.16, Na<sup>+</sup> = 39.75) and (b) NaI ( $\rho_{\text{max}}$  for water = 231.15, I<sup>-</sup> = 84.88, Na<sup>+</sup> = 32.40) in water. (c) Electrostatic potentials as a function of the distance from Au(111) surface for pure water, 3.87 M NaBr and 3.87 M NaI in water.

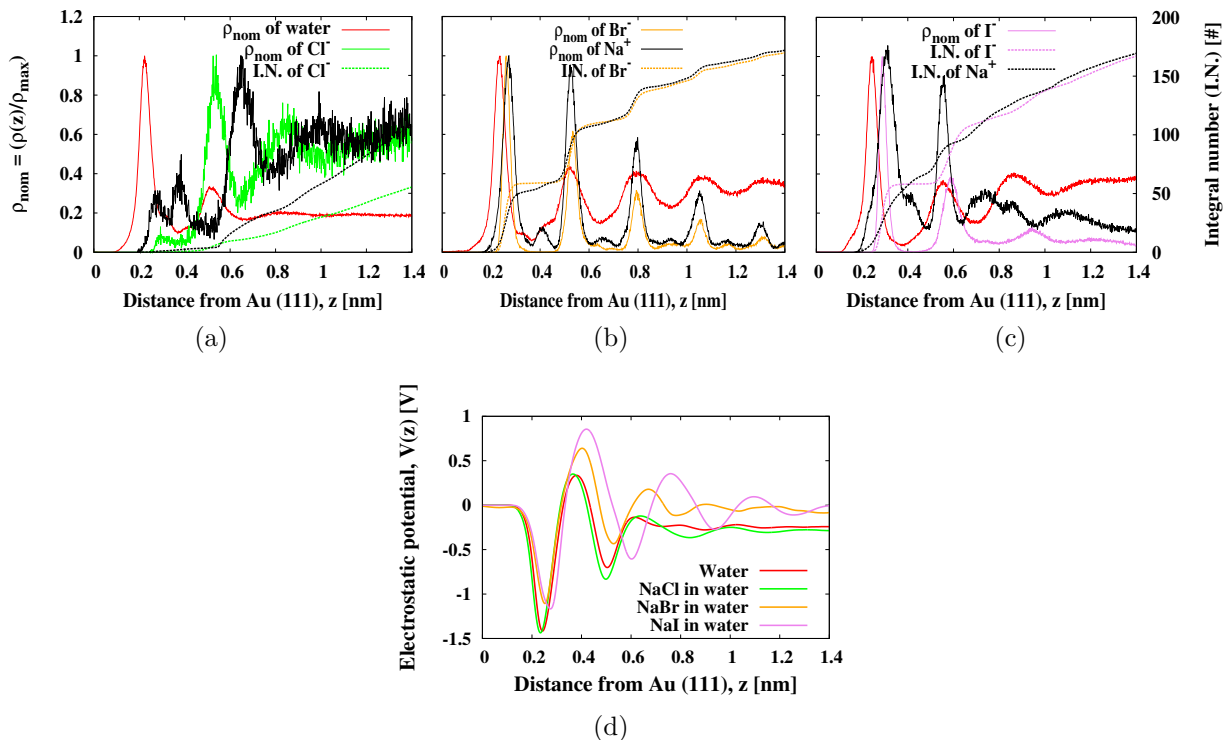


Figure S4: Normalized ion densities (number densities) of water and ions and integral numbers of ions as a function of the distance from Au(111) surface for 7.78 M (a) NaCl ( $\rho_{\text{max}}$  for water = 136.49,  $\text{Br}^-$  = 4.64,  $\text{Na}^+$  = 4.25), (b) NaBr ( $\rho_{\text{max}}$  for water = 249.13,  $\text{Br}^-$  = 97.63,  $\text{Na}^+$  = 54.58) and (c) NaI ( $\rho_{\text{max}}$  for water = 198.12,  $\text{I}^-$  = 91.81,  $\text{Na}^+$  = 34.13) in water. (d) Electrostatic potentials as a function of the distance from Au(111) surface for pure water, 7.78 M NaCl, 7.78 M NaBr and 7.78 M NaI in water.

# Details of the model for 100% CTAB on gold surfaces in water.

Models consisting of the electrolyte solutions containing 100% CTAB (2M solution), a mixture of 50% CTAB and 50% CTAC (1M CTAB, 1M CTAC), a mixture of 25% CTAB and 75% of CTAC (0.5 M CTAB, 1.5 M CTAC) and a 100% CTAC (2M solution) have been prepared for the gold nanorod surfaces Au(111), Au(110) and Au(100). Each of these models consists of a gold slab in contact with the surfactant layer and the electrolyte solution (as shown in Figure S5). Details of these simulation models, including box sizes, number of atoms, are reported in the main text in Table 2. Figure S5 shows the initial configuration for 100% CTAB on Au(111), which consists of a CTAB bilayer on both sides of the gold slab and bromide ions (orange) in water. The system was prepared by placing a CTAB bilayer on both sides of the gold slab in a simulation box. The preassembled system was then solvated with SPC waters. The bromide ions were added to the system by randomly replacing water molecules. The initial arrangement of the surfactant has been chosen based on the experimental suggestion that CTAB molecules are adsorbed on gold nanorods in the form of a bilayer. The initial surface density (packing density) of CTAB headgroup (CTA<sup>+</sup>) in the bilayer was chosen as 2.70 ions/nm<sup>2</sup>. This value is slightly larger than the surface density of 2.44 ions/nm<sup>2</sup> obtained for a square lattice with a radius of the CTAB headgroup of 0.32 nm<sup>2</sup> and close to the surface density of 2.83 ions/nm<sup>2</sup> obtained for an hexagonal lattice. Similar initial configurations were also used for the 100% CTAB on the Au(110) and Au(100) surfaces.<sup>5</sup>

## Convergence of the surface density with time

We have simulated the systems with 100% CTAB in water up to 200 ns. The convergence of the simulation results has been checked by calculating the surface densities of CTA<sup>+</sup> and

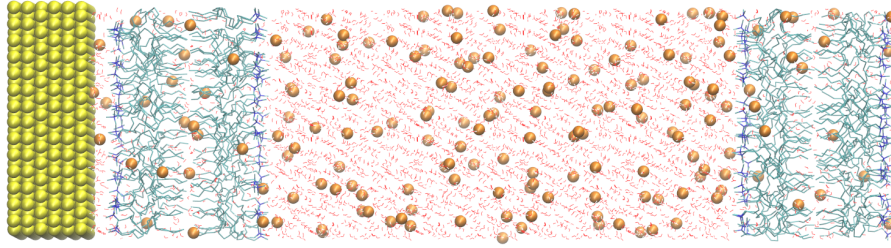


Figure S5: Initial configuration to start the simulation for 100% CTAB on Au(111) surface in water.

$\text{Br}^-$  as a function of time (Figure S6a), which are stable over the considered time window.

For the CTAB/CTAC mixtures and the pure CTAC, longer simulation times up to 1000 ns have been considered to allow for the system equilibration. Figure S6b shows the surface densities of  $\text{CTA}^+$  and  $\text{Br}^-$  as a function of time for 100% CTAC.

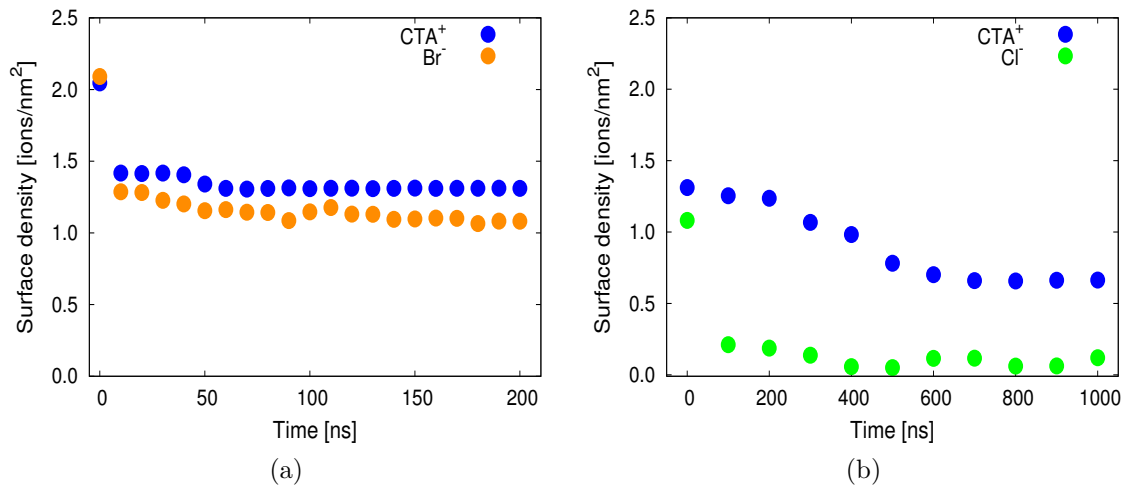


Figure S6: (a) Surface densities of  $\text{CTA}^+$  and  $\text{Br}^-$  as a function of time for 100% CTAB on Au(111) (b) Surface densities of  $\text{CTA}^+$  and  $\text{Cl}^-$  as a function of time for 100% CTAC on Au(111) surface

# Density profile and electrostatic potential profile for different CTAB/CTAC systems

The normalized number density of water,  $\text{CTA}^+$  and  $\text{Br}^-$  along with the integral numbers for the Au(111), Au(110) and Au(100) surfaces in contact with the 100% CTAB solutions are reported in Figure S7a, S7b and S7c, respectively.

Table S4: Potential difference,  $\Delta V$  between bulk and adsorbed surfactant layer on gold surfaces.

Name of surface	Au(111)	Au(110)	Au(100)
$\Delta V$ with 100% CTAB [V]	0.86	0.83	0.82
$\Delta V$ with 50% CTAB 50% CTAC [V]	0.57	0.56	0.57
$\Delta V$ with 25% CTAB 75% CTAC [V]	0.50	0.58	0.49

The electrostatic potential as a function of the distance from different gold surfaces is also included and presented in Figure S7e for 100% CTAB in water. In the case of the Au(110) interface a few water molecules can come quite close to the surface since they can adsorb in the void between gold atoms (see red solid line in Figure S7b). Also, the first peak in the density profile of  $\text{Br}^-$  ions is closer to the surface in the case of Au(110) than in the case of Au(111) and Au(100) as  $\text{Br}^-$  can better fit on the less dense Au(110) surface. The Au(100) surface represents an intermediate situation, where some more space is available for the ion absorption with respect to the closely packed Au(111) case, but less space is available with respect to the Au(110) case (see red solid line in Figure S7c). In the Au(100) interface the position of the first peak in the  $\text{Br}^-$  density profile is intermediate between that on Au(110) and that on Au(111) (dashed orange line in Figure S7a-c). Finally the  $\text{CTA}^+$  density profile (blue line in Figure S7a, S7b and S7c) follows the  $\text{Br}^-$  profile, which means that  $\text{CTA}^+$  ions adsorb next to  $\text{Br}^-$  ions.

In Figure S8 we report the normalized density profile of water,  $\text{CTA}^+$ ,  $\text{Br}^-$  and  $\text{Cl}^-$  along with the corresponding integral numbers (Figure S8a, S8b and S8c) for the 50% CTAB and 50% CTAC surfactant solution. A snapshot from the simulation of the Au(111) interface is

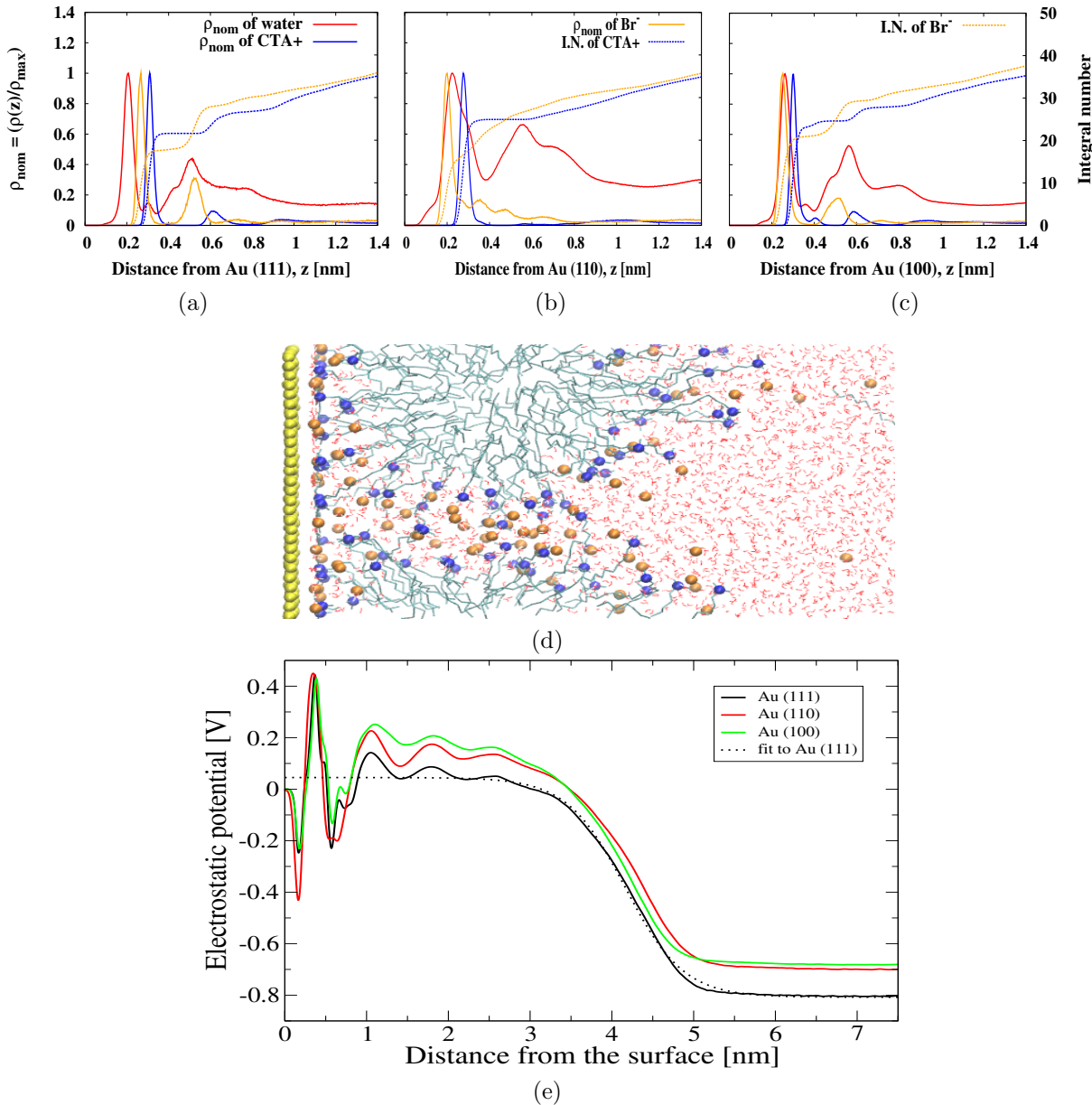


Figure S7: Normalized ion densities (number densities) of water and ions and integral numbers of ions as a function of the distance from (a) Au(111) ( $\rho_{\text{max}}$  for water = 179.26, CTA<sup>+</sup> = 36.74 Br<sup>-</sup> = 25.36), (b) Au(110) ( $\rho_{\text{max}}$  for water = 85.53, CTA<sup>+</sup> = 34.67, Br<sup>-</sup> = 19.56) and (c) Au(100) ( $\rho_{\text{max}}$  for water = 170.25, CTA<sup>+</sup> = 37.63, Br<sup>-</sup> = 27.76) in water. (d) Snapshot from simulations containing CTAB layer on Au(111) in water (e) Electrostatic potentials as a function of the distance from different gold surfaces for 100% CTAB in water.

also reported (Figure S8d). Finally, the electrostatic potential as a function of distance from different gold surfaces is also included (Figure S8e). From Figure S8a, S8b and S8c we can see that the water density profile is similar to that of the 100% CTAB system. Also in this

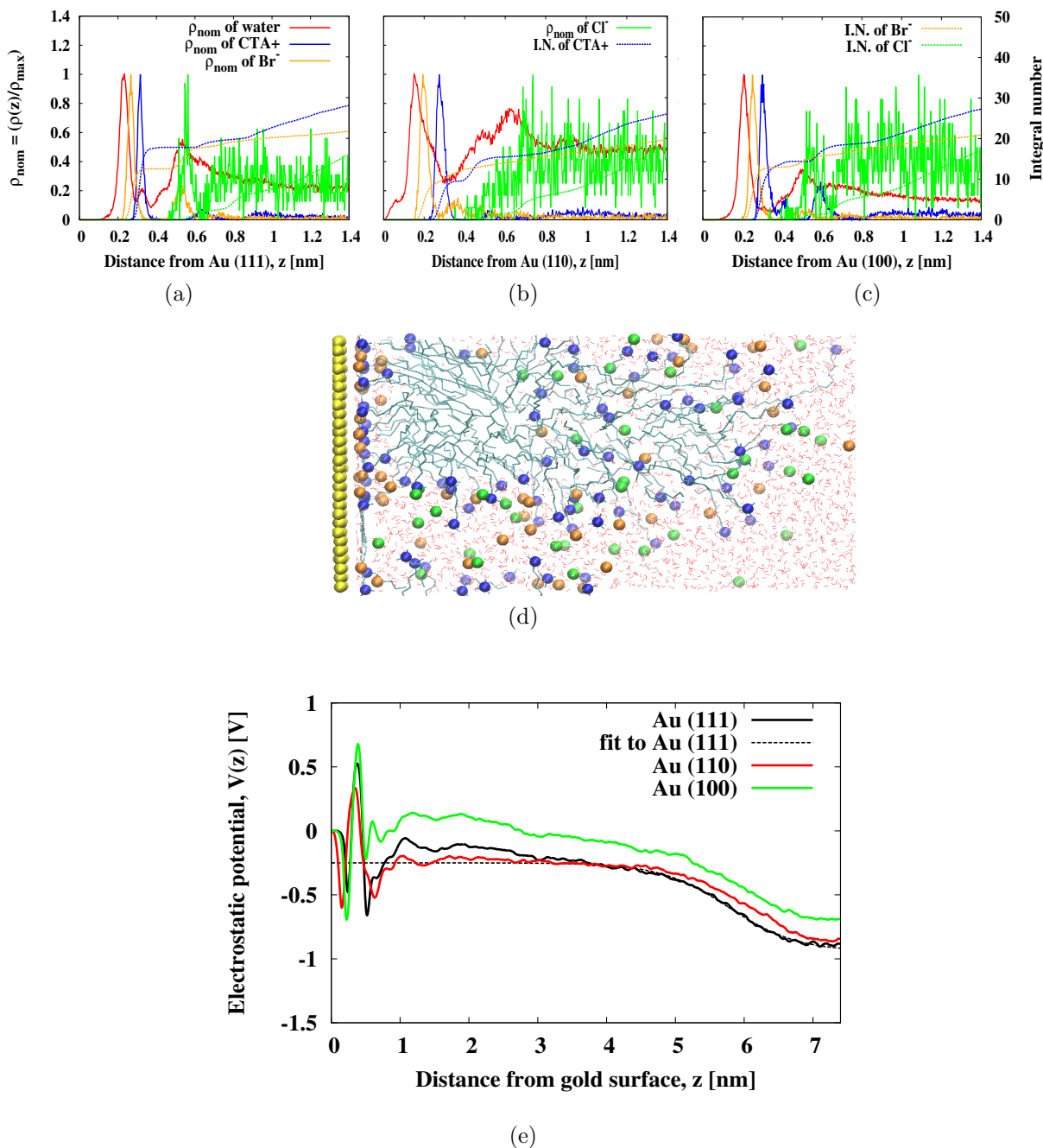


Figure S8: Normalized number densities (ion density) of water and ions and integral number of ions as a function of the distance from (a) Au(111) ( $\rho_{\text{max}}$  for water = 183.61, CTA<sup>+</sup> = 35.19, Br<sup>-</sup> = 22.32, Cl<sup>-</sup> = 1.57), (b) Au(110) ( $\rho_{\text{max}}$  for water = 103.73, CTA<sup>+</sup> = 22.00, Br<sup>-</sup> = 15.83, Cl<sup>-</sup> = 1.16) and (c) Au(100) ( $\rho_{\text{max}}$  for water = 297.46, CTA<sup>+</sup> = 19.24, Br<sup>-</sup> = 22.20, Cl<sup>-</sup> = 0.88) in water. (d) Snapshot from simulations containing 50% CTAB 50% CTAC layer on Au(111) in water. (e) Electrostatic potentials as a function of the distance from different gold surfaces for 50% CTAB and 50% CTAC mixture in water.

case, the water density profile for the Au(110) interface shows that some water molecules can be adsorbed in the void available between the gold atoms on the surface.  $\text{Cl}^-$  has negligible adsorption on the surface (in any of the three considered surfaces). Indeed the first peak of  $\text{Cl}^-$  density profile is very small (see normalized value) or negligible as compared to the second peak (green solid line). The integral number of  $\text{Cl}^-$  is negligible near all the gold surfaces (green dashed line).

As for the other cases, normalized ion density profiles along with integral numbers of  $\text{CTA}^+$ ,  $\text{Br}^-$  and  $\text{Cl}^-$  for the Au(111), Au(110) and Au(100) interfaces (Figure S9a, S9b and S9c, respectively) are reported for the 25% CTAB and 75% CTAC system. A snapshot from the simulation of the Au(111) interface is reported in Figure S9d and the electrostatic potential as function of the distance from different gold surfaces is also reported in Figure S9e.

Table S5: Average thickness of surfactant layer on different gold surfaces for different concentration ratio of CTAB/CTAC. The maximum standard error in the layer thickness is 0.05 nm.

Name of surface	Au(111)	Au(110)	Au(100) [nm]
100% CTAB	3.86	3.74	3.85
50% CTAB 50% CTAC	5.87	6.10	5.98
25% CTAB 75% CTAC	5.97	6.03	6.05
100% CTAC	1.80	2.40	1.80

Figure S10 shows the normalized density profile of water,  $\text{CTA}^+$  and  $\text{Cl}^-$  along with the integral numbers. A snapshot from the simulation of 100% CTAC solution on the Au(111) surface (Figure S10d) and the electrostatic potential as a function of distance from the different gold surfaces for 100% CTAC system are also reported (Figure S10e). The integral number of  $\text{CTA}^+$  for Au(111), Au(110) and Au(100) show that about 30 surfactant molecules are adsorbed on the Au(111) (namely 11 molecules in the first layer and 19 molecules in the second layer), about 40 surfactant molecules are adsorbed on Au(110) (11 molecules in the first layer and 29 molecules after first layer) and 24 surfactant molecules are adsorbed on the

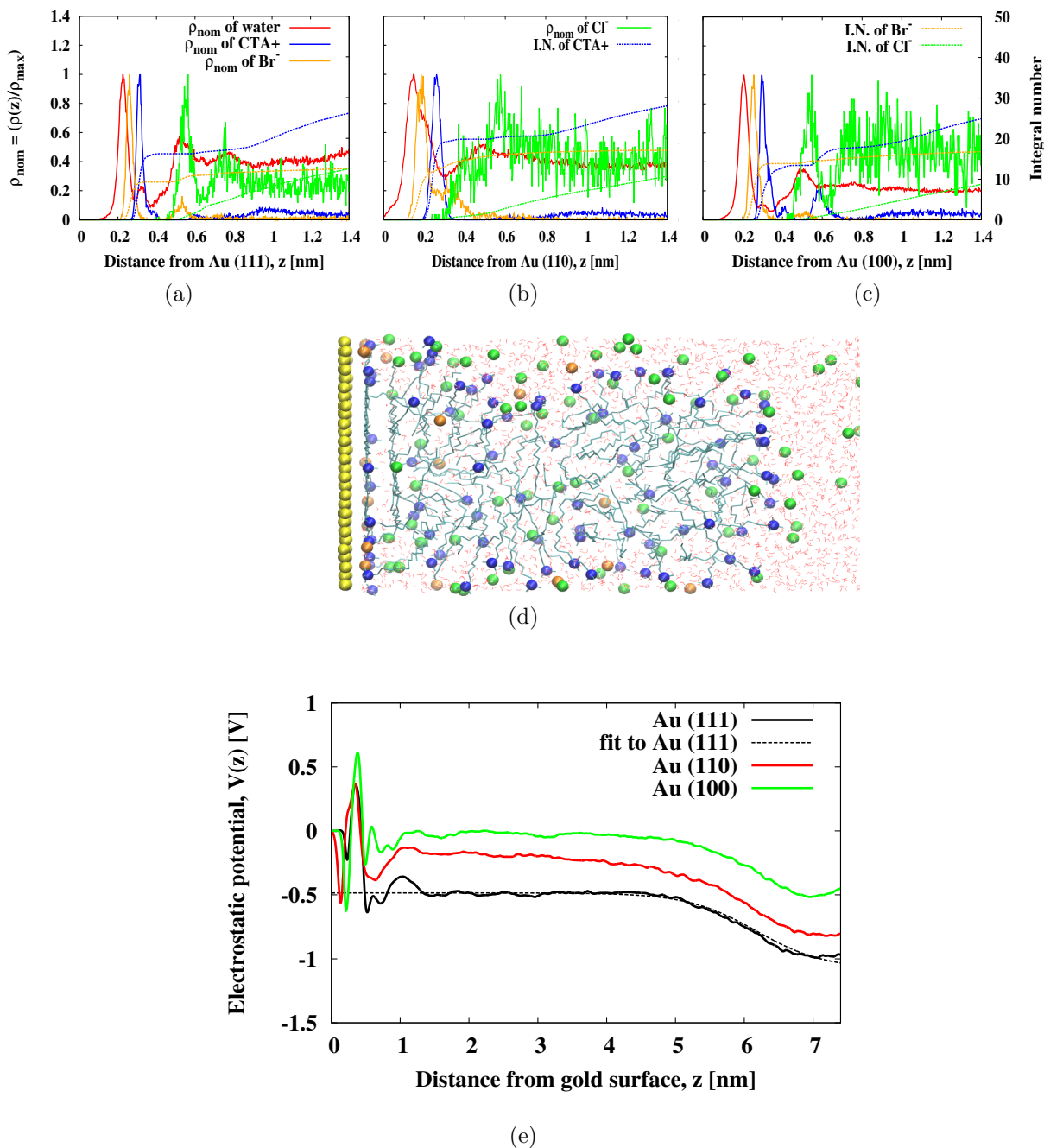


Figure S9: Normalized ion density (number density) of water and ions and integral number of ions as a function of the distance from (a) Au(111), ( $\rho_{\text{max}}$  for water = 114.10, CTA<sup>+</sup> = 21.42, Br<sup>-</sup> = 12.20, Cl<sup>-</sup> = 3.03) (b) Au(110) ( $\rho_{\text{max}}$  for water = 123.82, CTA<sup>+</sup> = 20.00, Br<sup>-</sup> = 10.00, Cl<sup>-</sup> = 1.47) and (c) Au(100) ( $\rho_{\text{max}}$  for water = 255.79, CTA<sup>+</sup> = 17.57, Br<sup>-</sup> = 18.03, Cl<sup>-</sup> = 1.36) in water. (d) Snapshot from simulations containing 25% CTAB 75% CTAC layer on Au(111) in water. (e) Electrostatic potentials as a function of the distance from different gold surface for 25% CTAB and 75% CTAC mixture in water.

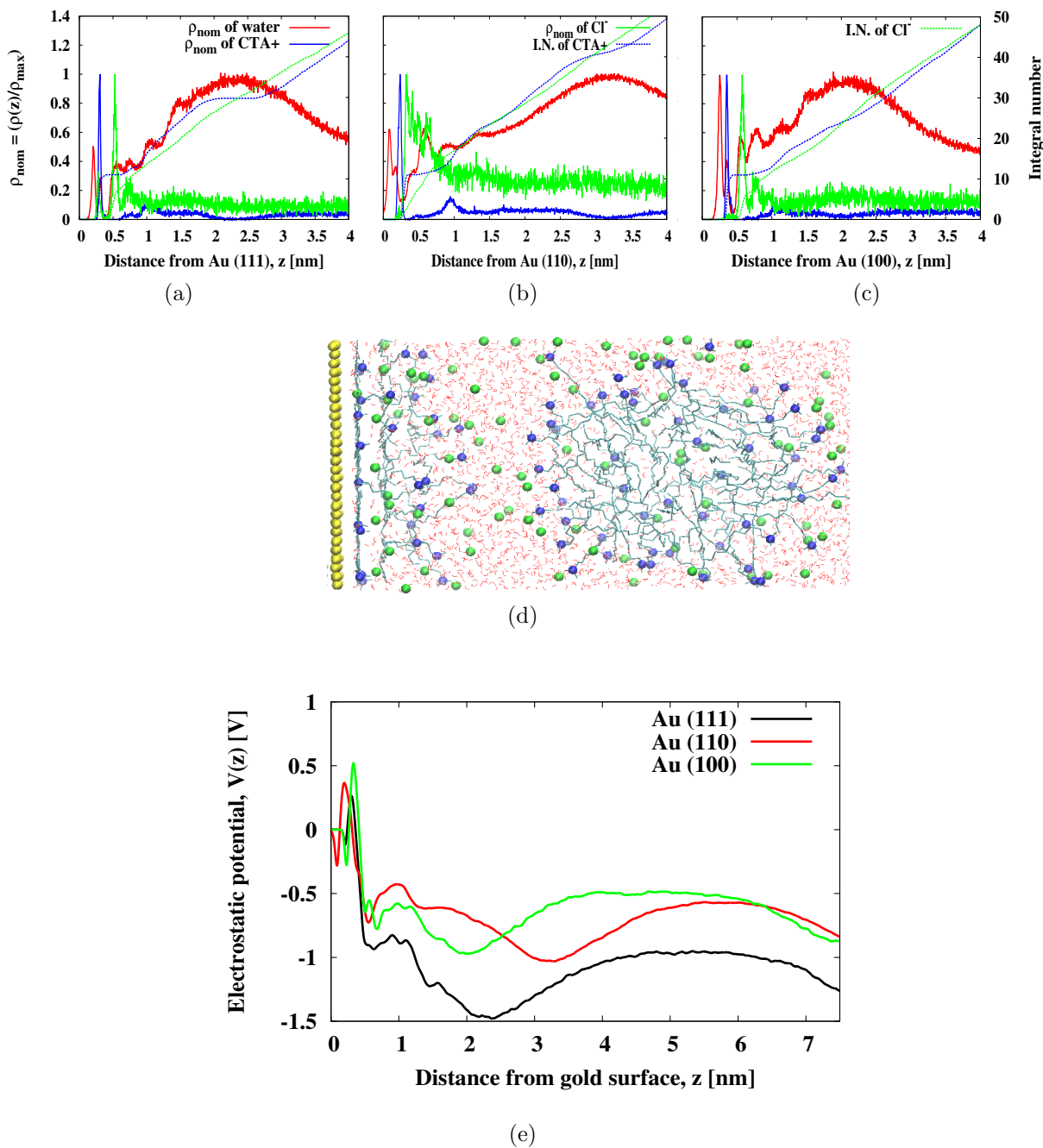
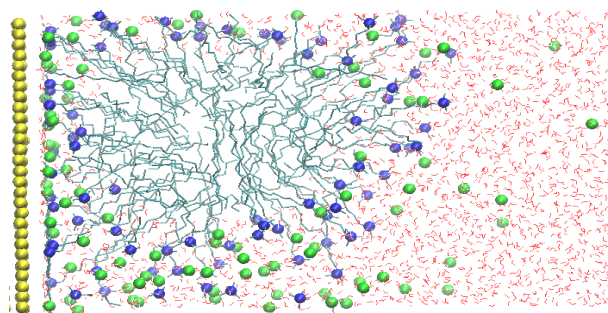
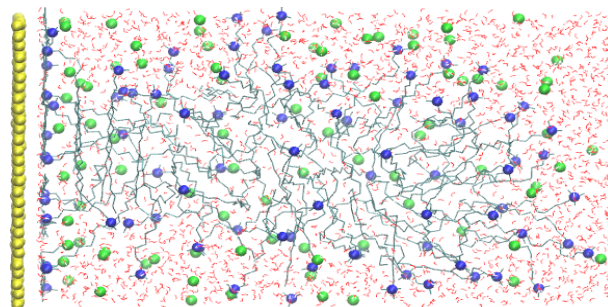


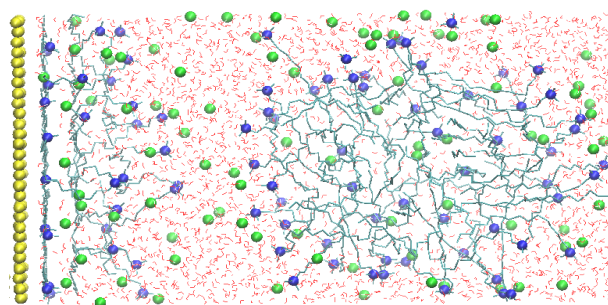
Figure S10: Normalized ion densities (number densities) of water and ions and integral number of ions as a function of the distance from (a) Au(111) ( $\rho_{\text{max}}$  for water = 110.90, CTA<sup>+</sup> = 18.20 Cl<sup>-</sup> = 6.36), (b) Au(110) ( $\rho_{\text{max}}$  for water = 110.9, CTA<sup>+</sup> = 12.13, Cl<sup>-</sup> = 2.47) and (c) Au(100) ( $\rho_{\text{max}}$  for water = 102.96, CTA<sup>+</sup> = 15.24, Cl<sup>-</sup> = 5.50) in water. (d) Snapshot from simulation containing CTAC layer on Au(111) in water (e) Electrostatic potentials as a function of the distance from different gold surfaces for 100% CTAC in water.



(a)



(b)



(c)

Figure S11: Snapshots from simulations containing CTAC layer on Au(111) in water at (a)  $t = 0$ , (b)  $t = 300$  ns and (c)  $t = 600$  ns

Au(100) (namely 11 molecules in the first layer and 13 molecules in the second layer). The detached micelles for the Au(111), Au(110) and Au(100) interfaces consist of 60, 50 and 66 surfactant molecules respectively. Figure S11 shows the detachment of the CTAC micelle from the Au(111) surface as function of time. We have started with our simulation at time  $t = 0$  (Figure S11b) with a CTAC micelle adsorbed on the gold surface (Such a system has been obtained starting from a CTAB micelle adsorbed on the gold surface where the  $\text{Br}^-$  ions have been replaced by  $\text{Cl}^-$  ions). As the simulation proceeds the CTAC micelle stretches out towards the solution (Figure S11b). Finally, the CTAC micelle detached from the gold

surface (Figure S11c).

The average density of CTA<sup>+</sup> as a function of distance from different gold surfaces is presented in Figure S12 for 100% CTAB, 50% CTAB and 50% CTAC, 25% CTAB and 75% CTAC and 100% CTAC systems, respectively. Figure S12 and Table S5 show that the thickness of the surfactant layer increases with the increase of the CTAC concentration, which also means that the surfactant layer becomes less compact.

## Conversion of plasmon shift to layer thickness

To interpret the experimental determined resonance shift  $\Delta\lambda_{\text{res}}$ , i.e. converting the plasmon shifts to a change in layer thickness, we use equations and parameters determined solving the Maxwell equations, where we use available values of the bulk dielectric functions for the materials. The Maxwell equations were solved numerically using the Boundary Element Method (BEM). To a good approximation, the plasmon shift for gold nanorods induced by an adsorption layer with refractive index  $\Delta n$  higher than the surrounding medium and thickness  $t$ , is given by:<sup>6</sup>

$$\Delta\lambda = S\Delta n(1 - e^{-\frac{t}{d_{\text{sens}}}}). \quad (2)$$

In this equation,  $S$  is the sensitivity and  $d_{\text{sens}}$  the sensing distance, i.e. the distance at which a layer causes  $(1 - \frac{1}{e})$  of the maximum shift. The sensitivity  $S$  depends on the particles. For the particles we used here, the sensitivity was determined experimentally as  $S = 143.1$  nm/RIU.<sup>7</sup> From a large set of simulations, we have found that the sensing distance  $d_{\text{sens}}$  is well approximated as:

$$d_{\text{sens}} = 0.37V^{(\frac{1}{3})}. \quad (3)$$

where  $V$  is the nanorod's volume.<sup>8</sup> Our particles had a length of  $a = (67.8 \pm 9.2)$  nm and a width  $b = (31.1 \pm 5.6)$  nm.<sup>7</sup> With these parameters, we calculated the plasmon shift  $\Delta\lambda_{\text{res}}$  as a function of layer thickness  $t$  and its refractive index (Figure S15). The data shown in

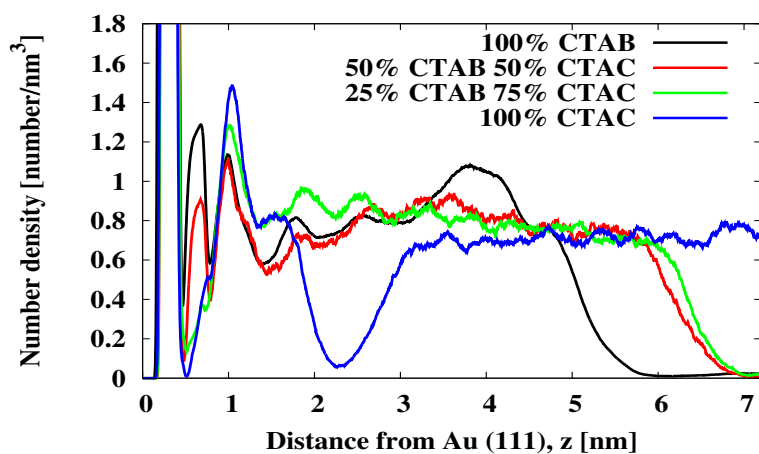
Figure S15 allows us to convert the measured shifts in plasmon resonance wavelength to a change in layer thickness using a refractive index of the surfactants CTAB of  $n = 1.4^{9,10}$  and assuming the same refractive index for CTAC. These conversions result in a layer thickness of 1.6 nm for CTAC and 4.2 nm for CTAB, in good agreement with the results from the molecular dynamics simulations.

---

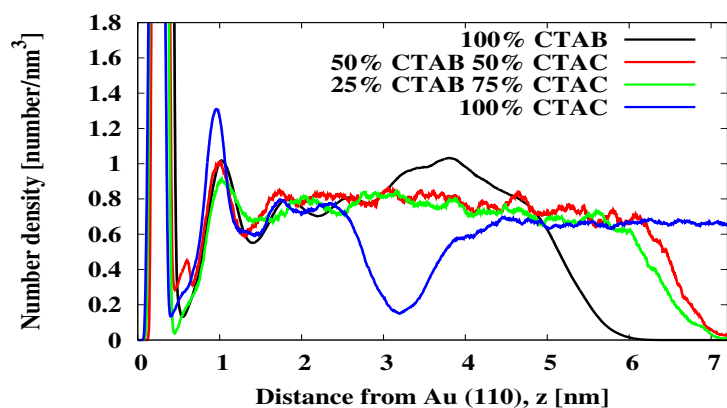
## References

- (1) D'Angelo, P.; Migliorati, V.; Guidoni, L. Hydration Properties of the Bromide Aqua Ion: the Interplay of First Principle and Classical Molecular Dynamics, and X-ray Absorption Spectroscopy. *Inorg. Chem.* **2010**, *49*, 4224–4231.
- (2) Patra, M.; Karttunen, M. Systematic Comparison of Force Fields for Microscopic Simulations of NaCl in Aqueous Solutions: Diffusion, Free Energy of Hydration, and Structural Properties. *J. Comput. Chem.* **2004**, *15*, 678–689.
- (3) Marcus, Y. Ionic Radii in Aqueous Solutions. *Chem. Rev* **1988**, *88*, 1475–1498.
- (4) Gurtovenko, A. A.; Vattulainen, I. Calculation of the electrostatic potential of lipid bilayer from molecular dynamics simulations: methodological issue. *J. Chem. Phys.* **2009**, *130*, 215107–215114.
- (5) Meena, S. K.; Sulpizi, M. Understanding the microscopic origin of gold nanoparticle anisotropic growth from molecular dynamics simulations. *Langmuir* **2013**, *29* (48), 14954–14961.
- (6) Nusz, G. J.; Curry, A. C.; Marinakos, S. M.; Wax, A.; Chilkoti, A. Rational Selection of Gold Nanorod Geometry for Label-Free Plasmonic Biosensors. *ACS Nano* **2009**, *3*, 795–806.
- (7) Rosman, C.; Prasad, J.; Neiser, A.; Henkel, A.; Edgar, J.; Sönnichsen, C. Multiplexed

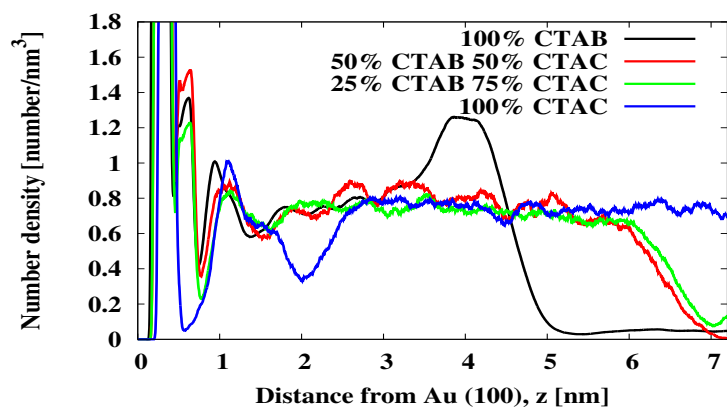
- plasmon sensor for rapid label-free analyte detection. *Nano Lett.* **2013**, *13*(7), 3243–3247.
- (8) Henkel, A. *Rod-shaped plasmonic sensors : synthesis and single particle spectroscopy.*; Universität Mainz, Zentralbibliothek, 2014; p XII 125 S.
- (9) Ashkarran, A. A.; Bayat, A. Surface plasmon resonance of metal nanostructures as a complementary technique for microscopic size measurement. *Int. Nano Lett.* **2013**, *3*, 50–60.
- (10) Yu, C.; Varghese, L.; Irudayaraj, J. Surface modification of cetyl tri methyl ammonium bromide-capped gold nanorods to make molecular probes. *Langmuir* **2007**, *23*, 9114–9119.



(a)



(b)



(c)

Figure S12: Averaged ion density (number density) of  $\text{CTA}^+$  as a function of distance from (a) Au(111), (b) Au(110) and (c) Au(100) surfaces for 100% CTAB, 50% CTAB and 50% CTAC, 25% CTAB and 75% CTAC and 100% CTAC systems.

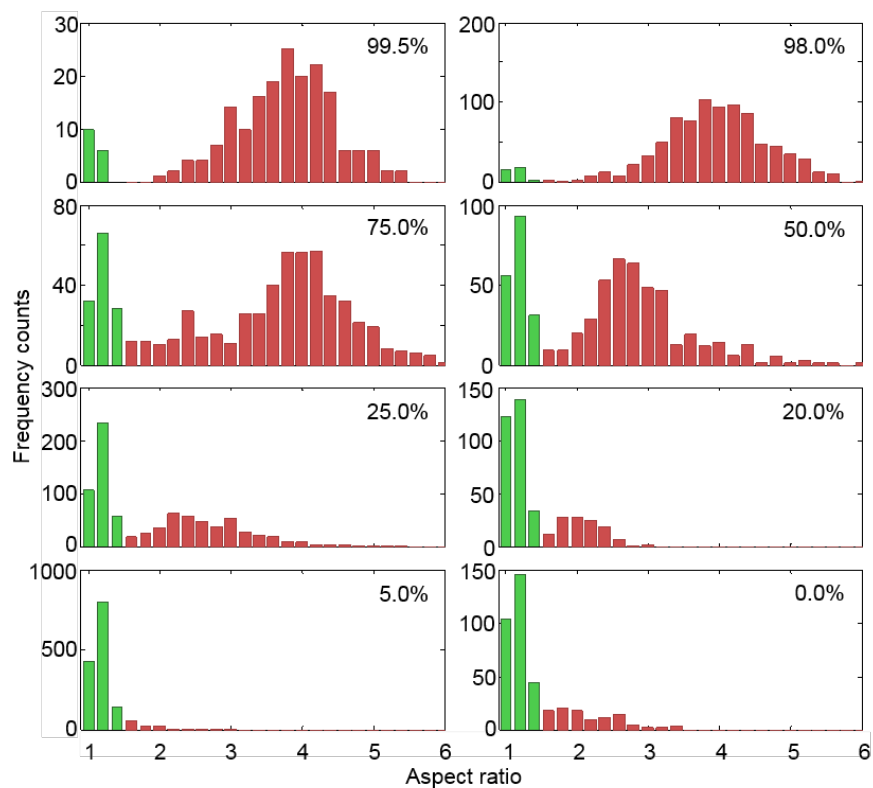


Figure S13: Histogram of particle dimensions determined from TEM images of the nanoparticles produced with different ratios of CTAB and CTAC, given in percentage of CTAB (upper right corner). To distinguish spherical (green) and rod-shaped particles (red), we used a cutoff value of 1.5. The ratio of spheres to rods is described in the main text.

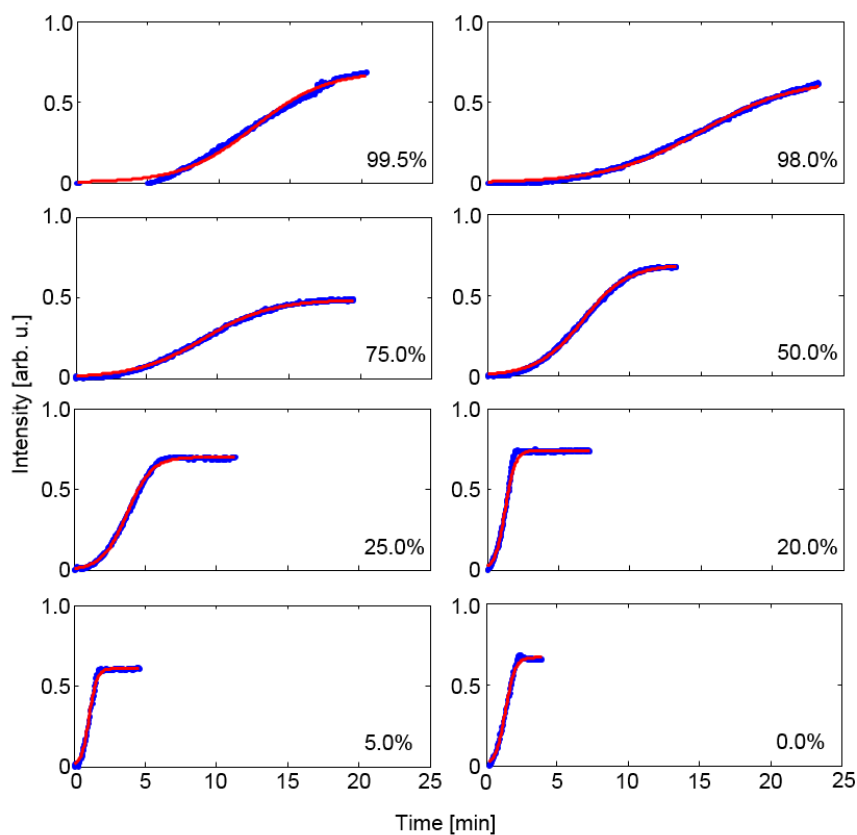


Figure S14: Growth kinetics extracted from the absorbance spectrum in the interband region at 450 nm as a function of time for growth solutions with different CTAB to CTAC ratios, given in percentages of CTAB. The experimental data (blue dots) has been fitted with a Boltzmann function (solid red line) to extract the reaction rate constants for each solution. The figure shows increasing reaction speed with decreasing percentage of CTAB as predicted by simulation.

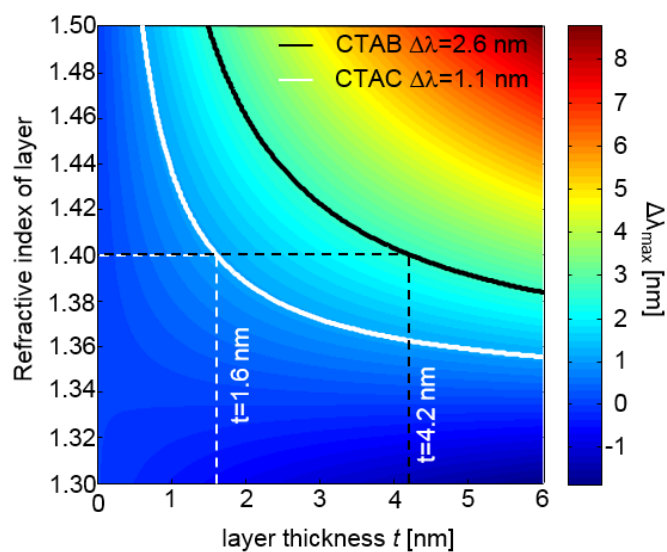


Figure S15: Calculated resonance shift  $\Delta\lambda_{\text{res}}$  for different values of layer thickness and refractive index. Solid black and white lines show contours for experimentally determined resonance shifts of CTAB and CTAC layers. Dotted black and white lines represent the conversion from resonance shift to layer thickness of CTAB and CTAC using published values for the refractive index of CTAB ( $n=1.4$ ).<sup>9,10</sup>